

ON THE PRESSURE DISTRIBUTION BETWEEN SOLID SURFACES IN CONTACT

TAKAO KATO, SHINOBU KATO and KATSUMI YAMAGUCHI

Department of Mechanical Engineering

(Received October 31, 1980)

Abstract

A new method was developed to find the interface pressure distribution of metallic surfaces in contact by measuring the roughness change. The pressure distribution of two kinds of contact surfaces, a sphere and a flat surface, a flat end of a cylinder and a flat surface, was measured experimentally by the method and compared with that of the elasticity theory. As a result, it was shown that it is possible to find the pressure distribution by measuring the roughness change in the contact surface before and after contact.

1. Introduction

The pressure distribution between various machine components in contact such as a bolted joint on a machine tool has a close relation to the stiffness of the joint and greatly influences the behaviour of machine tools or the machining accuracy. It is thus of great interest and practical importance to find the pressure distribution between rough surfaces in contact in discussing the problem of friction, wear and lubrication in engineering practice. Much research has thus been devoted for many years to finding the distribution of contact stress between elastic bodies pressed against one another.

Theoretically, many workers¹⁻³⁾ have reported solutions based upon the theory of elasticity, commencing with the classical studies by Hertz⁴⁾. However, these have been limited to the simple case of the two-dimensional or the axi-symmetrical problem. Recently, with the development of computer analysis, the Point-Matching Method⁵⁾ or Finite Element Method⁶⁾ has been used to obtain the pressure distribution of the contact surfaces, which has not been elucidated fully yet.

Experimentally, three-dimensional photoelasticity techniques⁷⁾ and a pressure measuring method using ultrasonic waves⁸⁾ have been attempted in order to determine the pressure distribution between contact bodies, but it seems both leave much to be desired in the way of accuracy.

In the present study a new experimental method has been developed for measuring easily the pressure distribution between actual metallic bodies in contact by using the changes in the surface roughness encountered before and after contact.

2. Method of Measuring Pressure Distribution

When two metallic bodies are pressed together, real contact occurs at certain discrete tips of the asperities on the surface, because all engineering surfaces have asperities larger than a molecule. However carefully polished, in engineering practice, it is very difficult to prepare perfectly flat surfaces. Such fine asperities on the surface may deform plastically, causing a modification of surface roughness, even if the bulk materials deform elastically. The principle of measuring the pressure distribution in the present study derives from the fact that the changes in the surface roughness caused by the plastic deformation of asperities on the surface might be closely connected with the pressure distribution encountered, that is, the real area of contact of an asperity could be directly proportional to the load applied to it.

Now consider the case of contact between two metallic bodies, one that is hard with a smooth surface, the other soft with a rough surface which has ridge-shaped asperities of constant height as shown in Fig. 1. The tips of the asperities on the surface deform plastically depending upon the localized pressure encountered at the point of contact, even if the bulk material of the soft metal deforms elastically under a load. Thus, the load applied is transmitted from one to the other only through the tips of the asperities, so the pressure at the point of contact should be very high, and equal to the mean yield pressure of asperities in order to support the load applied. When the load is removed, the bulk material recovers elastically, though the plastic deformation at the tips of the asperities is retained as shown in Fig. 1.

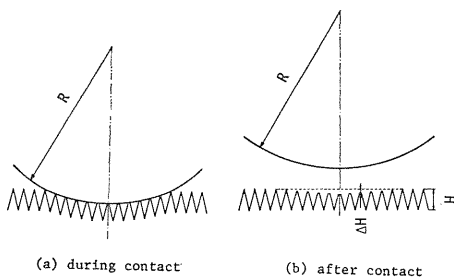


Fig. 1. Contact between a hard smooth surface and a soft rough surface.

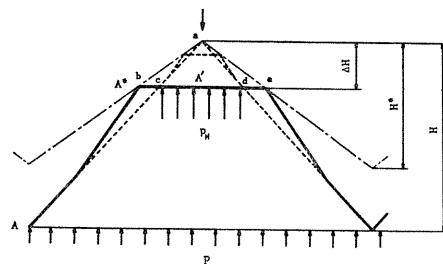


Fig. 2. Plastic deformation of a single asperity.

Next, consider the deformation of one asperity on the surface. Suppose a triangular asperity (not pyramidal but prismatic) of height H deforms plastically with a force applied as shown in Fig. 2 and that it deforms similarly in shape at every depression. If the apparent mean pressure acting on the surface cd is p_H , the area

of the surface cd is A' with the unit length considered perpendicular to the paper surface, the area of the bottom is A , and the apparent mean elastic pressure of the bulk material at the bottom of the asperity is p , then $pA = p_H A'$ from the equilibrium of force applied to the asperity. If the reduction in height of the asperity is ΔH , then from the geometrical similarity

$$p = p_H (A' / A) = p_H (\Delta H / H) \tag{1}$$

The mean pressure p at the bottom of the asperity is directly proportional to the change in height ΔH .

In the meantime, as the deformed material might flow outward as shown in Fig. 2 when the asperity is depressed by a flat, the real contact part is not the surface cd but the surface be . Even in this case, if the mean pressure at the depressed surface be is p_H^* , the mean pressure p at the bottom of the asperity is expressed as follows

$$p = p_H^* (A^* / A) = p_H^* (\Delta H / H^*) \tag{2}$$

where A^* is the area of the surface be , and H^* is the height of the asperity made by extending the line ae . That is, in both cases the mean pressure p at the bottom is directly proportional to the change in height ΔH .

Hereafter, for convenience equation (1) is used and the apparent yield pressure p_H (proportional constant) is obtained by calibration tests.

When the soft surface on which there exist regular triangular asperities of constant initial height H attains the roughness distribution $H(x, y)$ after making contact with the hard smooth surface, the pressure distribution encountered at the contact surface is generally expressed as follows

$$p(x, y) = p_H [H - H(x, y)] / H = p_H \Delta H(x, y) / H \tag{3}$$

H ; initial roughness

$\Delta H(x, y)$; roughness change

Then the load W applied can be calculated by integrating the pressure distribution $p(x, y)$ over the whole area of contact S (see Fig. 3) as the next equation.

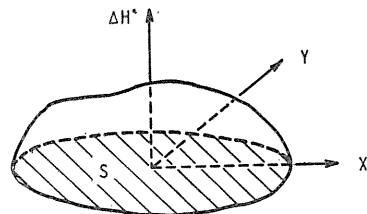


Fig. 3. Distribution of roughness change ΔH .

S : contact surface

$$W = \iint_S p(x, y) \, dx \, dy = p_H \iint_S \Delta H(x, y) / H \, dx \, dy \tag{4}$$

S ; area of contact

Therefore, if the apparent mean yield pressure p_H of the asperity is known, the pressure distribution and the load applied can be obtained from equations (3) and (4) respectively by measuring the changes in surface roughness before and after contact.

3. Experimental

In the present experiment the pressure distribution of two kinds of contact surfaces was investigated. A smooth sphere and a smooth flat ended cylinder were used as hard surfaces, each was pressed onto a soft flat surface with regular roughness, and the pressure distribution was measured experimentally by the proposed method. Hereafter, a hard surface will be called an indenter and a soft surface a specimen.

Indenters used here were quenched and lapped as flat and smooth as possible. The spherical indenter used was not a perfect sphere; one flat end of a cylinder (100 mm in radius, 100 mm in length) was machined to a spherical shape and finished with lapping. The diameter of the cylindrical indenter is the same as its height, (see Fig. 4)

The flat specimen which is pressed by the indenter is a cylinder made of carbon steel (150 mm in diameter), one flat end of which was finely grooved by turning on a lathe with a sharp sintered-carbide tool. The grooves were about 0.1 mm apart. In this way triangular prismatic asperities of constant height were formed on the surface of the specimen.

The size, material, hardness and other data of the indenter and specimen are listed in Table 1.

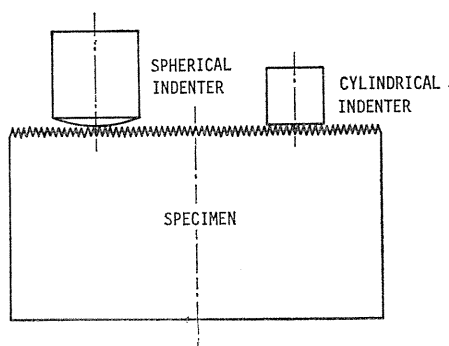


Fig. 4. Indenter and specimen.

Table 1. Indenter and Specimen

Shape	Indenter		Specimen
	Sphere	Cylinder	Flat surface of cylinder
Size	R420 R860 R1750	$\phi 5 \times 5$ $\phi 20 \times 20$	$\phi 150 \times 100$
Material	SKS2	SKS2	S35C
Heat Treatment	Quenching	Quenching	
Vickers Hardness Hv	750	630	210
Surface Roughness $R_{max} \mu m$	0.2	0.2	5~40

The loads were applied statically for about 20 seconds by means of a hydraulic universal testing machine.

4. Experimental results

Figure 5 shows an example of profilometer records of asperities machined on the specimen. The asperities are seen to be almost constant in height and nearly triangular in shape. However, in this experiment asperities were machined on the surface of the specimen by face turning, so strictly speaking, perfect triangular

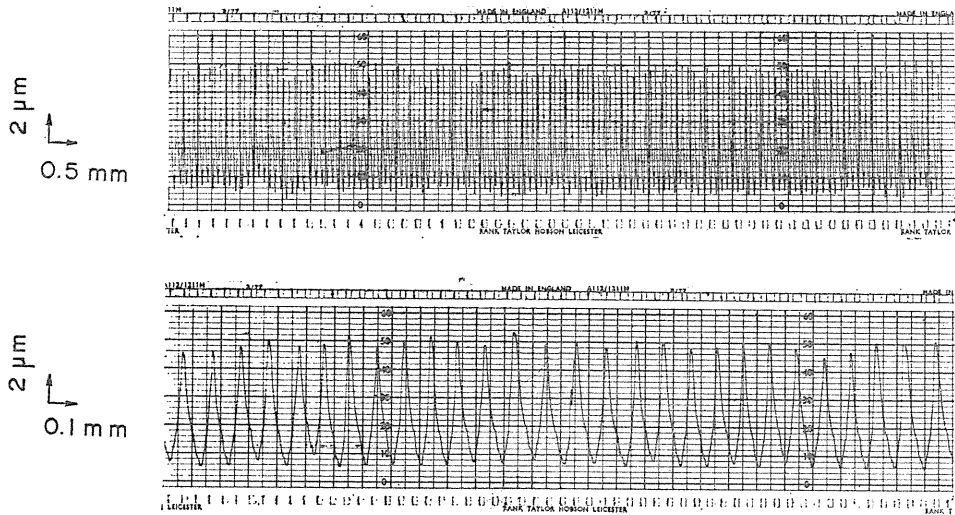


Fig. 5. Profilometer record of specimen.

prismatic asperities could not be obtained due to the roundness of the cutting edge. The asperities actually obtained are shown schematically in Fig. 6. Then if H' in this figure is regarded as the height of asperities, the depressed area (A' in Fig. 2) is overestimated compared with the case where H is used as the height. In practice, the plastic deformation of an asperity was confined to its upper part, and the real asperity was approximated by a triangle of height H by extending the upper sides of the asperity. Thus, H was used as the initial height in equations (3) and (4) instead of H' in Fig. 6.

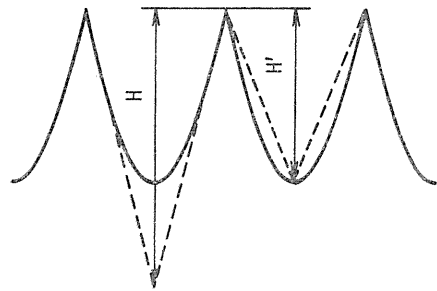


Fig. 6. Illustration of asperities.

The surface profiles of the spherical indenter and the cylindrical indenter used are shown in Figs. 7 and 8. The surface roughness of the indenters is very smooth (about $0.2 \mu\text{m}$); disregarding a few scratches, roughness is negligible compared with that of the flat specimens shown in Fig. 5. The roundness at the periphery of the flat end of the cylindrical indenter is also negligible.

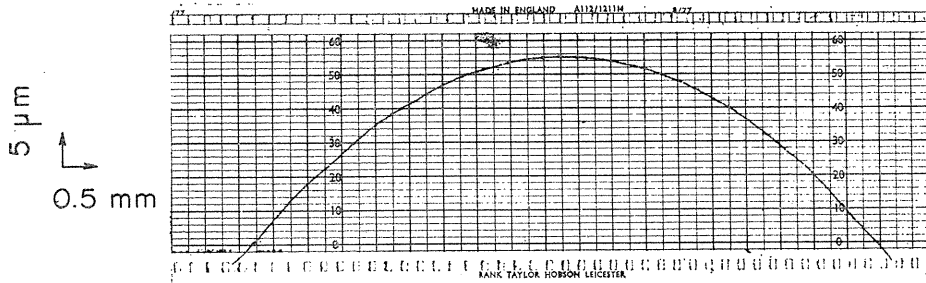


Fig. 7. Profilometer record of spherical indenter (420 mm in radius).

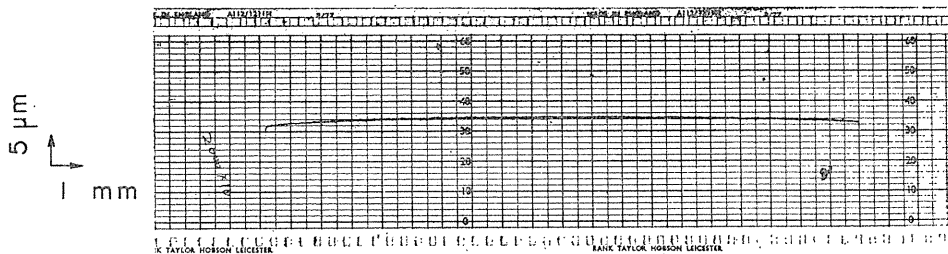


Fig. 8. Profilometer record of cylindrical indenter (20 mm in diameter, 20 mm in height).

Figure 9 shows an example of profilometer records of the surface of the specimen after pressing the spherical indenter (420 mm in radius) onto the specimen. The surface roughness was always measured perpendicular to the grooves. It is also noted that under the condition of Fig. 9 no plastic deformation in the bulk material has occurred, the plastic flow being confined to the tip of the asperities.

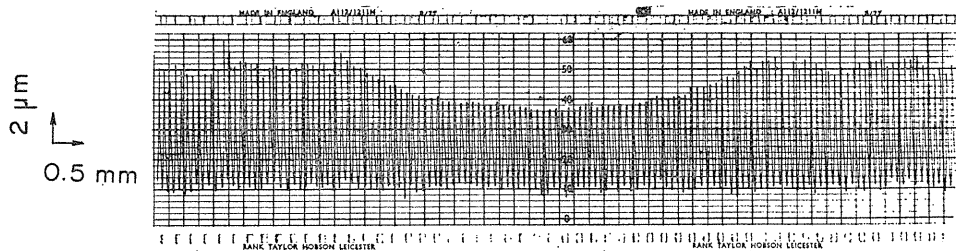


Fig. 9. Roughness change of specimen pressed by spherical indenter (420 mm in radius). $W=9.81\text{kN}$

Figure 10 shows the profilometer records of deformed asperities on the specimen surface when the flat end of the cylindrical indenter (20 mm in diameter) was pressed onto the specimen. It is noted from the figure that the plastic deformation of asperities is considerable at the periphery of the flat end of the cylinder, which results in a higher pressure.

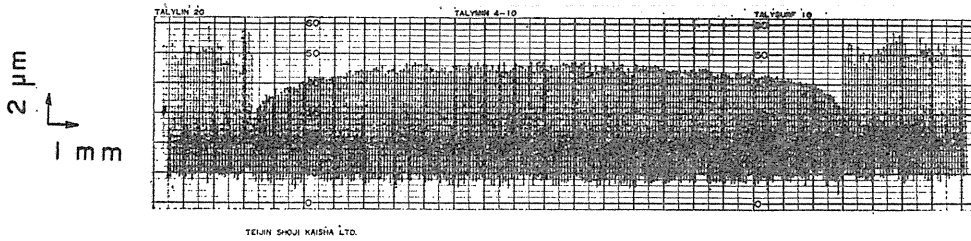


Fig. 10. Roughness change of specimen pressed by cylindrical indenter (20 mm in diameter). $W=98.1\text{kN}$

From the above traces, the changes in the surface roughness were obtained when two metallic bodies were placed in contact. Figure 11 shows the changes in surface roughness when the spherical indenter (1750 mm in radius) was pressed onto the specimen.

Figure 12 shows the changes in surface roughness when the flat end of the cylindrical indenter was pressed onto the specimen.

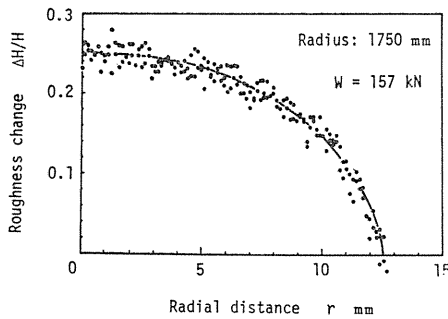


Fig. 11. Distribution of roughness change (sphere).

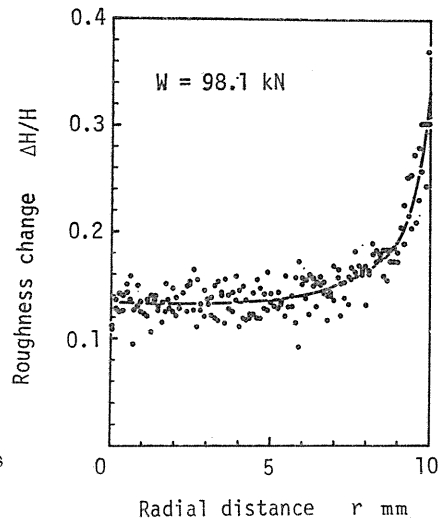


Fig. 12. Distribution of roughness change (cylinder).

An experimental point shown in Figs. 11, 12 is equivalent to a plastically deformed asperity on the specimen. As previously mentioned, the distribution of these points in the figures indicates the pressure distribution at the contact surface.

The numerical value of p_H must be known to obtain the pressure distribution quantitatively. Thus, it was calculated from equation (4) by carrying out the calibration test with known loads. The results indicate the numerical value of p_H is nearly 2060 MPa.

Generally, the real area of contact at the tips of the asperities has frictional as well as normal forces (see Fig. 13). It is necessary to check the effect of frictional force τ on the estimation of the pressure p . For this purpose, the pres-

pressure distribution between lubricated surfaces in contact was measured. In the case of dynamically loading or using lubricants of high viscosity, usually the lubricants are trapped between the asperities and bear a part of the load applied. In this experiment the pressure distribution under static contact where the lubricants bore no load was investigated. The contact area at the tips of the asperities could be regarded as being under boundary lubrication. It is noted from Fig. 14 that lubricants used had little influence upon the changes in surface roughness. It is seen then that within the limits of this measurement the numerical value of p_H is essentially independent of the lubricants used.

One example of the contact pressure distributions between the spherical indenter and the specimen is shown in Fig. 15; it was obtained from equation (3) by using the measured values of roughness changes $\Delta H/H$ mentioned above.

Figure 16 shows the pressure distribution for various initial roughnesses of the specimen and radii of the spherical indenter for a parameter of the relative roughness defined by the ratio of the initial roughness H of the specimen to the radius R

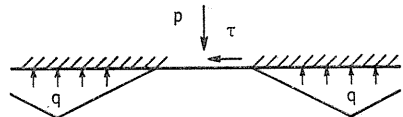


Fig. 13. Deformation of asperity.

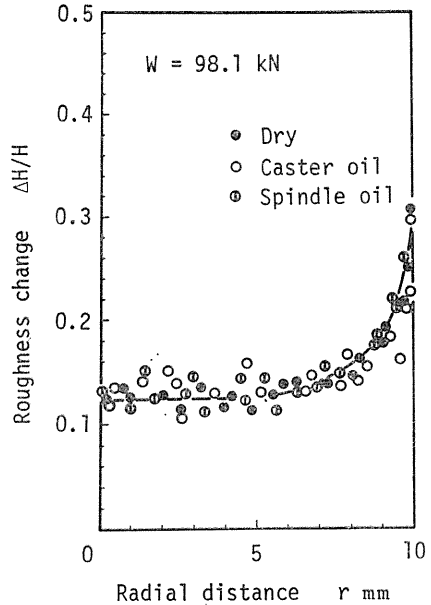


Fig. 14. Distribution of roughness change (cylinder).

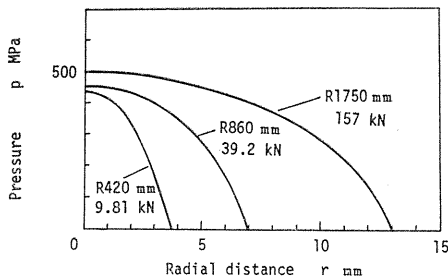


Fig. 15. Pressure distribution of spherical surface.

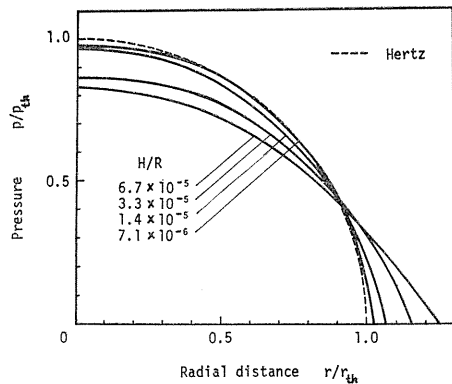


Fig. 16. Effect of relative roughness on pressure distribution.

of the spherical indenter. The abscissa indicates a nondimensional radial distance from the center defined by the ratio of the radial distance to the contact radius

r_{th} calculated by equation (5).

$$r_{th} = (0.75WR/E)^{\frac{1}{3}} \quad (5)$$

where $1/E = (1-\nu_1^2)/E_1 + (1-\nu_2^2)/E_2$

ν_1, ν_2 : Poisson's ratio for two surfaces

E_1, E_2 : Young modulus for two surfaces

R : radius of sphere

W : applied load

The ordinate indicates a nondimensional pressure defined by the ratio of the pressure measured p to the maximum pressure p_{th} calculated by equation (6),

$$p_{th} = 1.5W/\pi r_{th}^2 \quad (6)$$

The dotted line in the figure shows the pressure distribution calculated by the Hertzian equation. It is seen from this figure that as the relative roughness H/R becomes smaller, or an ideal contact condition is approached in which the surface roughness is negligible, the pressure distribution is in better agreement with the theoretical one by Hertz.

The following conclusions are obtained from these facts.

- (1) If the relative roughness is sufficiently small ($H/R \simeq 10^{-6}$), the pressure distribution can be obtained in the case when an ideally smooth surface is placed in contact.
- (2) If the relative roughness is a little larger ($H/R \simeq 10^{-5} \sim 10^{-4}$), the pressure distribution measured is considerably different from the Hertzian distribution. But the measured pressure distribution indicates the actual one encountered, even though it is different from the theoretical one. Therefore, when the surface roughness is large, it might be wrong to use the Hertzian pressure distribution.
- (3) Generally, when the relative roughness is large, the pressure around the center becomes low and the contact area becomes large.

One of the contact pressure distributions is shown in Fig. 17. The flat end of the cylindrical indenter (5 mm in diameter) is being pressed onto the specimen. The theoretical value represented by a dashed line is the Boussinesq's solution in the case where a flat end of a rigid cylinder is pressed onto an elastic half-space. The experimental results are in good agreement qualitatively with the theory in that the pressure is low around the center of the cylinder and increases abruptly towards the periphery. The difference in quantity between the experiment and the theory comes from the fact that the cylinder is assumed to be rigid in the theory, whereas the cylindrical indenter deforms elastically to a great extent in the experiment. It appears, then, that if the elastic deformation of the cylinder decreases, the elastic cylindrical indenter is approximately regarded as a rigid body and measured results closer to the theoretical ones could be obtained.

Then, in order to reduce the elastic deformation of the cylindrical indenters, the experiment was carried out with a short cylindrical indenter (2 mm in height). The result is shown in Fig. 18. In the figure the ordinate represents the nondimensional pressure defined by the ratio of the pressure p to the mean pressure p_m , and the abscissa represents the nondimensional radial distance defined by the ratio of the radial distance from the center r to the radius r_0 of the indenter. The

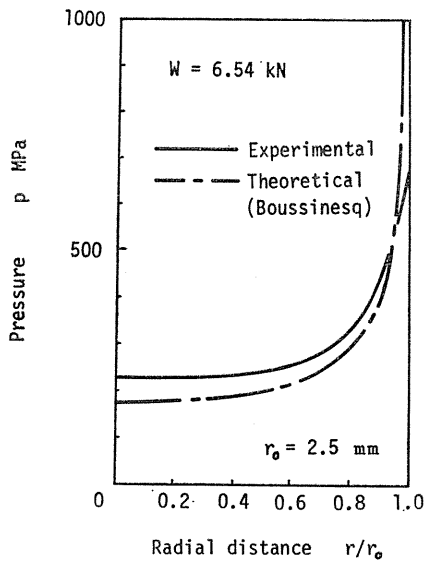


Fig. 17. Pressure distribution of a flat end of the cylindrical indenter (2.5 mm in radius).

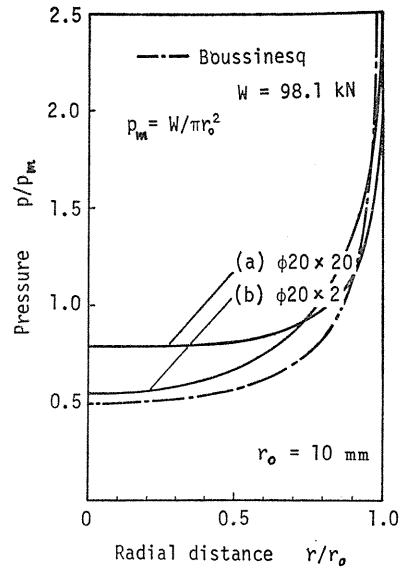


Fig. 18. Pressure distribution of a flat end of the cylindrical indenter (10 mm in radius).

dot-dash-line indicates the Boussinesq's theoretical solution. The curve (a) shows the pressure distribution for the cylindrical indenter (20 mm in height, 20 mm in diameter) being pressed onto the specimen, while the curve (b) shows the pressure distribution for the short cylindrical indenter (2 mm in height, 20 mm in diameter). It is shown that the curve (b) agrees closely with the theory compared with the curve (a).

For the two kinds of contact surfaces mentioned above, the pressure distribution measured by this method under a suitable condition is almost in agreement with the theoretical one, which means it is a reasonable method for measuring the contact pressure by means of the roughness change.

2. Discussion

The following points about this new method for measuring the contact pressure deserve discussion.

Firstly, one of the points is to estimate the apparent yield pressure p_H . According to the slip-line theory of rigid-plastic material advanced by Hill⁹⁾ the depressed area A^* increases by about 50% more than the area A' when there is no friction between contact surfaces and the apex angle of the asperity is about 130° . Since the depressed area is considered to be A' in Fig. 2 when there is large enough friction between them, it is to be expected that the real depressed area A^* takes the value (1~1.5) A' depending upon the friction. Then equation (2) is expressed as follows

$$p = p_H^*(A^*/A) = (1 \sim 1.5) p_H^*(A'/A) = (1 \sim 1.5) p_H^*(\Delta H/H) \quad (7)$$

In the experiment wherein the deformation of asperities is relatively small ($\Delta H/H < 0.33$) and individual asperity behavior is independent of the deformation of neighboring asperities, the deformation condition is similar at every depression if the frictional condition at the contact surface is constant. Then, the mean pressure p is directly proportional to the depression of asperity $\Delta H/H$ as expressed in equation (7). The proportional constant takes the numerical value between $(1 \sim 1.5) p_H^*(=p_H)$ depending on the friction at the contact surface.

According to the experiment by Bishop¹⁰⁾, the relation of $p_H^* \simeq 0.85 p_V$ is obtained where p_V is the yield pressure when pressing a pyramidal indenter of 68° semi-angle onto the flat surface, which is equivalent to the Vickers hardness, and p_H^* is the yield pressure of the asperity of semi-angle 70° being pressed by a flat. By using the above relation, the mean pressure p mentioned above is expressed as $p = (0.85 \sim 1.3) p_V (\Delta H/H)$. Then it is expected that it is reasonable to use the approximate relation $p = p_V (\Delta H/H)$ under the normal frictional condition. In fact, it was shown that the proportional constant is nearly equal to the Vickers hardness by the calibration test with a known force.

On the other hand, it is important to find which value between 0.85 and 1.3 should be used in order to calculate the pressure, since the proportional constant is different depending on the friction. Comparing the experimental results of lubricated surfaces with those of unlubricated surfaces (see Fig. 14), it is seen that within this experiment the friction has little influence upon the constant. This is because p_H/H is approximately equal to p_H^*/H^* , for though the depressed area increases and then H^* becomes small under the low frictional condition, p_H^* also becomes small as H^* becomes small.

Even with a material capable of workhardening, the deformation condition of the asperities of constant apex angle is considered to be similar whatever their depression¹¹⁾ as shown in Fig. 2, so it follows that the proportional relation between the mean pressure and the change in height can be applied.

The second problem is that the configuration of the contact surface is practically altered by the flattening of the tips of asperities. This is also the problem that the elastic deformation the underlying material with surface roughness undergoes differs to a certain degree from that in the case of contact with a smooth surface having no roughness. Let us consider this problem with reference to the contact between the sphere and the flat surface as shown in Fig. 19. For simplicity assume the sphere to be a smooth and rigid body. Then, compared with an ideal flat surface with no asperities, the elastic deformation of the bulk material decreases by the part shown by the hatching in Fig. 19 (a) disregarding the elastic deformation of an asperity, since the tip of the asperities deforms plastically. This means a modification of the configuration of the flat surface. The ratio of the elastic deformation d_e to the plastic deformation d_p of the

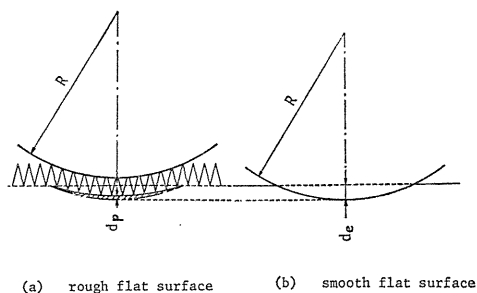


Fig. 19. Contact of sphere with flat surface.

asperity at the center of the contacting surface as shown in Fig. 19 is about 30% in the case of the contact of the specimen ($H=28.3\mu\text{m}$) with the sphere (420 mm in radius) ($W=102\text{N}$, $H/R=6.7\times 10^{-5}$). In this case the plastic deformation of the asperity cannot be negligible in comparison with the elastic deformation of the bulk material. Under such a condition the pressure distribution obtained by this method is equivalent to that of the contact of a concave specimen of a modified radius with a sphere. That is, the distribution differs from the Hertzian distribution of an ideal smooth surface pressed by a smooth sphere with the same radius of 420 mm in that the pressure at the central area is lower and the contact radius is larger (see Fig. 16). Nevertheless, it must be remembered that the pressure distribution obtained by this experiment indicates precisely the pressure distribution encountered at the actual contact surface with asperities existing on it, though the distribution is different from the Hertzian distribution of the ideal surface. Accordingly, when the plastic deformation of asperities on the contact surface is relatively large, it is wrong to assume the Hertzian pressure distribution.

On the contrary, in the case of the contact of a flat surface ($H=6.4\mu\text{m}$) with a sphere of 1750 mm radius ($W=1632\text{N}$, $H/R=7.1\times 10^{-6}$), the ratio of d_e to d_p is about 6%, and the pressure distribution is in good agreement with the Hertzian one of an ideal surface as shown in Fig. 16. That is, if the ratio of the plastic deformation of the asperity to the elastic one of the bulk material is of such a degree, the effect of the plastic deformation of the asperity on the pressure distribution is almost negligible. And when the pressure distribution is measured experimentally with specimens of different roughnesses, the exact pressure distribution for an ideal surface will be obtained by means of the extrapolation.

The third problem is that the measurement of the pressure distribution is carried out discretely by using the plastic deformation of an asperity as a pressure measuring element. But it is apparent that the pressure at a very narrow part such as the edge of a flat end of the cylinder can be measured with sufficient accuracy since asperities with sufficiently small pitch can be made. It is also possible to measure the pressure at the much smaller part if a sufficiently large indenter is made.

This method makes use of the phenomenon that the real contact area of a deformed asperity is directly proportional to the load applied; thus it can be applied to any case only if the condition for proportionality is satisfied. Therefore the pressure distribution of a contact surface having any shape can be measured by this method. But it is necessary to apply enough load so as to be able to measure the plastic deformation of asperities by profilometer and, in order to assure satisfactory measuring accuracy, a plastic deformation of the asperities greater than the scatter of initial height is needed.

On the other hand, too much of a load will result in severe plastic deformation in the bulk material. In the case where the bulk material deforms plastically, this measuring method might also be applied if the approximate similarity of the deformation of the asperity is retained. However, this remains a problem for future investigation.

6. Conclusion

A new method is developed to ascertain the pressure distribution of metallic surfaces in contact by measuring the roughness change $\Delta H/H$. The pressure distribution of two kinds of contact surfaces, a sphere and a flat surface, a flat end of a cylinder and a flat surface, was measured experimentally by the proposed method and compared with that of the elasticity theory. The results may be summarized as follows.

- (1) It is possible to find the pressure distribution by measuring the roughness change in the contact surface before and after contact.
- (2) The method can be applied to a contact surface of any shape for which the pressure distribution has not been obtained by the elasticity theory.

Acknowledgement

The authors wish to thank the members of the Laboratory of Mechanical Engineering, Nagoya University, who generously assisted in the research work.

References

- 1) Sneddon, I. N., "The Elastic Stresses Produced in a Thick Plate by the Application of Pressure to its Free Surfaces," Proc. Camb. Philos. Soc., Vol. 42, 1946, pp. 260-271.
- 2) Greenwood, J. A., "The Elastic Stresses Produced in the Mid-plate of a Slab by Pressure Applied Symmetrically at Its Surface," Proc. Camb. Phil. Soc., Vol. 60, 1964, pp. 159-169.
- 3) Lardner, T. J., "Stresses in a Thick Plate with Axially Symmetric Loading," Journal of Applied Mechanics, Trans. ASME, Vol. 32, 1965, pp. 458-459.
- 4) Timoshenko, S. P., Goodier, J. N., Theory of Elasticity, McGraw-Hill, p. 409.
- 5) Conway, H. D., Vogel, S. M., Farnham, K. A., and So, S., "Normal and Shearing Contact Stresses in Indented Strips and Slabs," Int. J. Engng. Sci. Vol. 4, 1966, pp. 343-359.
- 6) Gould, H. H., Mikic, B. B., "Area of Contact and Pressure Distribution in Bolted Joints," ASME Journal of Engineering for Industry, 1972, Vol. 94, pp. 864-870.
- 7) Bradley, T. L., Lardner, T. J., and Mikic, B. B., "Bolted Joint Interface Pressure for Thermal Contact Resistance," ASME Journal of Applied Mechanics, 1971, Vol. 38, pp. 542-545.
- 8) Ito, Y., "A Contribution to the Effective Range of the Preload on a Bolted Joint," Proceedings of the 14th Int. MTDR Conf., 1973, pp. 503-507.
- 9) Hill, R., The Mathematical Theory of Plasticity, Oxford at the Clarendon Press, 1950. p. 221.
- 10) Bishop, R. F., Hill, R., and Mott, N. F., "The Theory of Indentation and Hardness Tests," Proc. Phys. Soc., 1945, Vol. 57, pp. 147-157.
- 11) Bowden, F. P., and Tabor, D., The Friction and Lubrication of Solids, Clarendon Press, London, 1954, p. 17.